ANALYSIS OF A TURBINE ROTOR CONTAINING A TRANSVERSE CRACK AT OAK CREEK UNIT 17

G. W. Rogers and C. A. Rau, Jr.
Failure Analysis Associates
Palo Alto, California 94303

J. J. Kottke and R. H. Menning
Wisconsin Electric Power Company
Milwaukee, Wisconsin 53201

SUMMARY

Transient increases in one, two and three per revolution vibration characteristics of a low pressure steam turbine were observed during steam temperature reduction operations. Vibration and fracture mechanics analyses suggested the presence of a transverse shaft crack which was eventually identified by ultrasonic inspection and confirmed by destructive sectioning. Signature analyses of vibration data recorded over a two-year period prior to crack identification are correlated with fatigue crack growth, which occurred intermittently during transient temperature decreases. The apparent increased response of the rotor to vibration is due to asymmetric stiffness changes introduced by the growing transverse crack. The vibration response is predicted to increase with increasing crack depths in excess of 10% of the shaft diameter. Fracture mechanics analyses predict that fatigue crack growth occurred during periods of steam temperature decrease, when high surface tensile stresses are present. These same transient thermal stresses are shown to have retarded and prevented subsequent fatigue crack growth during steady operation.

INTRODUCTION

Failure Analysis Associates (FAA) was retained by Wisconsin Electric Power Company (WEPCO) to analyze abnormal transient vibration levels observed during boiler deslagging operations of their Oak Creek Unit 7 320 MW General Electric turbine generator. Of particular interest were the vibration levels recorded on main bearing caps of the low pressure, 1800 rpm turbine/generator set.

Boiler deslagging was performed on this unit to dislodge slag that accumulated on the outside wall of water and steam tubes. The procedure calls for reduction in furnace firing rates which causes cooling in particular tube regions. Subsequent thermal contraction effectively dislodges mineral deposits.

The subject turbine/generator utilizes four journal bearings, one pair supporting each of the turbine and generator rotors. The vibration characteristics of the bearing caps monitored when the turbine/generator was at a fully loaded condition were essentially the same as those recorded during early stages of unit operation. Horizontal, vertical,and axial vibrations were recorded for each bearing cap. In addition, shaft rider sensors monitored vibration at an angle of approximately 25° from vertical.

VIBRATION ANALYSIS

Figure 1a is the normal steady state vibration signature obtained with a shaft rider probe at the number 1 turbine bearing. A strong synchronous 1800 rpm signal and very slight two and three per revolution signals are present. Figure 1b, on the other hand, shows the signature at peak vibration levels subsequent to a thermal down ramp of 140°F (77°C). Note the increase in the one, two, and three per revolution amplitudes.

The vibration characteristics of turbine bearings number 1 and 2 were similar. Both bearings exhibited a significant increase in synchronous and twice-synchronous signals during the transient temperature decrease.

A comparison of vibration data and other parameters indicated a correlation between steam temperature and vibration amplitude. It was observed that a decrease in steam temperature resulted in a delayed vibration level increase. Increases in steam temperature, on the other hand, either did not affect the vibration or reversed a vibration increase associated with a previous temperature decrease. As expected with thermally induced phenomena, there was a definite time lag between steam temperature change and the observed change in vibration. An example of the vibrational response associated with steam temperature variation is shown in Figure 2. Reduction in steam temperature cools the surface of the shaft relative to the shaft bore. This condition produces tensile hoop stresses and tensile axial stresses of sufficient magnitude that a transverse crack in the shaft near the surface would open. Such a crack was subsequently identified near the mid span of the double-flow rotor under the inlet edge of the first shrunk-on, turbine wheel of the governor end.

FATIGUE CRACK PROPAGATION ANALYSIS

Fractography of the cracked rotor shaft after removal from service showed the presence of a fatigue crack of size and shape illustrated by Figure 3. Fracture mechanics calculations of fatigue crack growth were performed by integration of the material's crack growth rate law over the range of crack driving forces to obtain the crack progression between some initial size and the final size.

The crack driving force is conveniently characterized by the crack tip stress intensity factor ΔK, which is proportional to nominal stress range $\Delta\sigma$, the square root of the crack size a, and the specific crack and part geometry. To compute the specific magnitude of the steady (K_s) and cyclic (ΔK) crack driving force for the crack shape modelled in Figure 3, we have utilized a general purpose fracture mechanics computer program BIGIF [1]. The crack driving forces (ΔK and K_s) for shaft bending are summarized in Table I. BIGIF was used to accurately compute K_s and ΔK for the more complex stress distribution near the shaft surface. This distribution is affected by the stress concentration associated with the diameter change, fillet radius, and shrunk-on disk contact stress. However, because these localized surface stresses affect the magnitudes of K_s and ΔK only for cracks near a surface, it was not necessary to compute their magnitude in order to quantify K_s and ΔK for the deeper crack depths between four and seven inches where vibration changes were introduced.

The rate of fatigue crack growth in rotors made from Ni-Cr-Mo-V low alloy steels has been studied by various investigators. The crack growth rate per cycle, da/dN

can be represented over a wide range of growth rates by a power law of the form

$$\frac{da}{dN} = C\ \Delta K^{\eta} \qquad (1)$$

where C is 5.99×10^{-10} for $K_{min}/K_{max} = 0$ and increases with increasing K_s; η is approximately 2.8. At low values of ΔK, the crack growth rate falls below that predicted by equation (1), and eventually a threshold value of $\Delta K = \Delta K_{th}$, is reached below which fatigue crack growth does not occur. The fatigue threshold, ΔK_{th}, is also dependent on the ratio of steady stress (σ) to cyclic stress ($\Delta\sigma$), or the ratio of K_s to ΔK. Specifically, Hopkins and Rau [2] have shown that the specific effect of the stress ratio, $R = \sigma_{min}/\sigma_{max} = K_{min}/K_{max}$, can be estimated as

$$\Delta K_{th}(R) = \frac{A-R}{B}\ \Delta K_{th}\ (R=0) \qquad (2)$$

where A and B are material constants and generally $A \simeq B \simeq 1.6$.

The nominal cyclic stresses during steady state operation are estimated by the manufacturer to be ± 1.6 ksi (or $\Delta\sigma = 3.2$ ksi). With a bearing misalignment of 0.050 inch, the nominal cyclic stresses will be $\Delta\sigma = 4$ ksi. The steady stress from centrifugal force and the small steady-state axial and radial thermal gradients should be near zero and probably less than 5 ksi. However, during the deslagging operation, the the steam temperature is quickly reduced by 100-150°F, and the shaft surface is cooled relative to the bore, setting up a radial temperature gradient which introduces surface tensile stresses up to $\sigma_s = E\ \alpha\ \Delta T = (30 \times 10^3) \times (6.6 \times 10^{-6}) \times 130^{\circ}F = 26$ ksi, where E = elastic modulus in ksi, α = coefficient of thermal expansion in inches per inch°F, and ΔT = change in temperature in °F.

Utilizing BIGIF, the crack driving force, ΔK, corresponding to $\Delta\sigma = 3.2$, was calculated for a range of crack depths. BIGIF was also used to numerically integrate equation (1) to obtain the increase in crack depth, a, caused by rotating bending during the periods of the high steady stresses produced during deslagging. The results are shown in Figure 4 for the case where C, in equation (1), is elevated by the high mean stress during the deslag cycle to 5.7 times the value at $K_{min}/K_{max} = 0$.

CRACK GROWTH THRESHOLD CONDITIONS

Because the 1800 rpm turbine speed introduces fatigue cycles very quickly (1800 x 60 min/hr x 24 hr/day = 2.6 million cycles per day), crack growth could not have been occurring continuously during normal operation. Otherwise the crack would have grown to a size where the rotor would have failed. The reason that cracking does not occur during normal operating conditions is that the ΔK produced is below the material's apparent threshold considering prior loading history. In the absence of any steady stress ($\sigma_s = 0$), the threshold of these rotor steels is typically between 6 and 10 ksi$\sqrt{in}$. Using a 6 ksi$\sqrt{in}$ threshold value, the cyclic nominal stress at which a 6.7 inch deep crack would grow is obtained from Table I and equation (2) to be $\Delta\sigma = 3.0$ ksi. Therefore, since the nominal cyclic stress of $\Delta\sigma = 3.2$ ksi with perfect bearing alignment is greater than this value, fatigue crack growth did not occur under steady-state operation in this case because the high steady stress which caused fatigue crack

growth during deslag also served as an overload, increasing the effective threshold above which fatigue crack growth can occur. Figure 5 shows published results of Hopkins, Rau, Leverant and Yuen [3]. These results indicate a major increase in the apparent threshold stress intensity factor, ΔK_{th}, when preceded by an overload. The larger the relative overload, the higher the apparent threshold for subsequent crack growth. In the case of the OC7 rotor, the ratio of maximum overload stress to maximum steady state stress is at least

$$\frac{26 + 1.6}{5 + 1.6} = 4.2$$

and perhaps as high as

$$\frac{26 + 1.6}{1.6} = 17.$$

The data of Figure 5 show that the corresponding apparent threshold for fatigue crack growth during turbine operation after a deslag cycle will be at least 1.6 times higher and may be more than five times higher than the threshold would have been without the deslag overload cycle. Specifically, the cyclic nominal stress above which the 6.7-inch crack can continue to grow when $\sigma_s = 0$, is between 1.6 x 3 = 4.8 ksi and 5 x 3 = 15 ksi. If steady-state operation produces some small tensile steady stress, the apparent threshold will be reduced by the factor computed by equation (2). Nevertheless, the magnitude of the overload produced by the deslag was sufficient to prevent continued propagation during subsequent steady operation.

CRACK GROWTH VS. VIBRATION INCREASE

The correlation of crack growth to changes in the vibration characteristics of the turbine rotor involves many factors. First it has been recognized [4,5,6,7,8] that a continuously open crack produces a twice per revolution rotor response due to a rotating, asymmetrical stiffness analogous to an elliptical shaft geometry. An opening and closing crack, on the other hand, may produce synchronous, two, three, four, and even higher multiples of synchronous responses due to the form of rotor orbit.

The nature of the crack and the state of stress associated with the thermal transients previously described suggest the the crack was, in fact, continuously open during the periods of high vibrational response. Grabowski, in particular, [9] has shown analytically that the change in shaft compliance and hence the dynamic response due to the asymmetry is relatively insensitive to crack size until the crack depth is approximately 10% of the shaft diameter.

As shown in Figure 2, the amplitude of the second harmonic vibration is near a maximum for a period of approximately three (3) hours. It was estimated that the crack is fully open for this period of time due to the state of transient thermal stress. The total number of deslag operations performed on the OC7 unit between installation and the time such procedures were eliminated was approximately 1100. Using the three (3) hour time estimate for each, the total number of high thermal stress state cycles can thus be calculated as

$$1100 \text{ cycles} \times 3 \text{ hours} \times \frac{1800 \text{ cycles}}{\text{min.}} \times \frac{60 \text{ min.}}{\text{Hr.}} = 356 \times 10^6 \text{ cycles} \qquad (3)$$

The calendar period over which these cycles occurred was reviewed and correlated to

recorded maximum increase in vibration during selected deslag operations. The form of the recorded data is unfiltered peak to peak displacement, in mils, as sensed on the number 1 bearing cap in the vertical direction. A curve fit of these data as a function of cycles under the thermal transient conditions as calculated in equation (3) is shown in Figure 6. Figure 7 shows the correlation of the maximum change in low-pressure turbine bearing cap vibration during deslag with predicted rotor crack growth.

The graph shows that the point at which the change in vibration becomes recognizable corresponds to a crack depth between 3 and 4 inches: or between 8% and 10% of the shaft diameter. This correlates very well with the crack depth (10% of rotor diameter) predicted analytically by Grabowski [9] as necessary for significant increase in rotor vibration response.

At the time of this writing, sufficient data reduction to establish similar time history amplitude curves for individual synchronous and twice-synchronous components of the unfiltered bearing cap vibration data has not been completed. Figure 2, however, shows an example of expected differences between the first and second harmonics. Whereas the absolute magnitude of change in velocity for the two harmonics is of the same order, the percentage change in the second harmonic is much greater than in the first harmonic.

Vibration data for certain rotor coast downs were also recorded on magnetic tape. Bode plots of amplitude vs. frequency for first, second, and third harmonics of rotor speed were generated as shown in Figure 8. Note that the ordinate is a logrithmic scale of velocity. The first critical speed was observed to be approximately 1035 cpm. The second and third harmonics responded at 1050 and 1080 cpm, respectively, most probably due to the increase in stiffness in the bearing oil film with reduced rotor speed.

MODIFIED UNIT OPERATION

Acting upon an initial belief that the rotor contained a transverse crack, but prior to actual determination of that fact by inspection, WEPCO decided to continue operation with revised procedures. This decision was based primarily on the fact that steady-state, full-load operation showed no trend towards vibration increase and the conclusion that the crack was propagating only during the deslag cycles as previously discussed.

The operating procedures were therefore modified to minimize high vibrations and hence to minimize the magnitude of thermal down ramps. This was accomplished by limiting the unit to a constant 200 MW output, regardless of system demand. At the 200 MW load, the boiler slagging is minimized, thereby eliminating the need for continual deslagging cycles.

The procedure for taking the unit off line was also revised since it was believed desirable to have crack closure while coasting down through critical speeds. This was accomplished by keeping the shaft at approximately constant temperature. The method employed brought the unit to a minimum load until vibration returned to normal after which the load was dropped rapidly while maintaining high steam temperatures.

The result of these procedures was that the trend of continually increased vibration level with age or deslag cycles ceased. Also, no increase in steady-state vibration

was observed. These operating restrictions continued until the unit was shut down, ultrasonically inspected, and the rotor removed for repair.

SUMMARY AND CONCLUSIONS

Some vibrational characteristics of a large steam turbine rotor containing a transverse crack have been identified. It was determined that the measured vibration signatures during thermal transient deslag operations correspond to analytically predicted responses for a continuously open crack. The vibration signatures also showed significant increase in the twice per revolution response of the rotor and an overall vibration amplitude increase with increasing crack depth.

Fracture machanics analysis, including the effects of prior "overloads" on subsequent fatigue crack growth, was used to predict crack growth. The increase in bearing cap vibration was correlated with the predicted crack growth. This trend compared very well with the analytically predicted onset of rotor response to stiffness asymmetry caused by a growing transverse crack near the mid span of a rotor. It was shown that a crack depth corresponding to approximately ten percent of the shaft diameter is necessary to produce a significant change in the rotor vibration response.

Although there are many factors which affect rotor vibration response to cracking (such as axial position of the crack or the phase relationship of the crack to rotor eccentricity), it has been shown that vibration monitoring, rotor dynamics analysis, and fracture mechanics analysis can be used to identify, predict and understand the presence and growth of transverse cracks in large steam turbine rotors.

REFERENCES

1. Besuner, P.M., Rau, S.A., Davis, C.S., Rogers, G.W., Grover, J.L., and Peters, D.C., "BIGIF: Fracture Mechanics Code for Structures--Introduction and Theoretical Background - Manual 1," EPRI NP-1830, April 1981.

2. Hopkins, S.W., and Rau, C.A., Jr., "Prediction of Structural Growth Behavior Under Fatigue Loading," Fatigue Crack Growth Measurements and Data Analysis, ASTM STP 783, 1981.

3. Hopkins, S.W., Rau, C.A., Jr., Leverant, G.R., and Yuen, A., "Effect of Various Programmed Overloads on the Threshold for High-Frequency Fatigue Crack Growth," Fatigue Crack Growth Under Spectrum Loads, ASTM STP 595, 1976.

4. Grabowski, B., "The Vibrational Behavior of a Turbine Rotor Containing a Transverse Crack," Transactions of the ASME, Vol. 102, January 1980.

5. Mayes, I.W., Crack Propagation in Rotating Shafts, ASME 77-DET-164.

6. Mayes, I.W., and Davies, W.G.R., The Vibrational Behavior of a Rotating Shaft System Containing a Transverse Crack, I. Mech. E. C168/76.

7. Okah-Avae, B.E., Analogue Computer Simulation of a Rotor System Containing a Transverse Crack, Simulation, Dec. 1978.

8. Zrebarth, H., and Baumgartner, B.J., Early Detection of Cross-Sectional Rotor Cracks by Turbine Shaft Vibration Monitoring Techniques, 81-JPGC-Pwr-20.

9. Grabowski, B., "The Vibrational Behavior of a Rotating Shaft Containing a Transverse Crack -- Part 1 - Crack Models and the Vibration of a Rotor with Single Disk on a Massless Shaft Containing a Transverse Crack," (to be published) 1982.

TABLE 1. - NORMALIZED CRACK DRIVING FORCE FOR CHORD CRACK IN CIRCULAR SHAFT UNDER LINEAR STRESS VARIATION (BENDING)

Crack Depth (inches)	K/σ $(\Delta K/\Delta\sigma)$	ΔK (for $\Delta\sigma$ = 3.2 ksi) (ksi $\sqrt{in}$)	K_s (for σ_s = 25 ksi) (ksi $\sqrt{in}$)
0.99	1.395	5.02	34.88
1.98	1.940	6.98	48.50
2.80	2.235	8.05	55.88
4.00	2.630	8.42	65.75
5.60	2.990	9.57	74.75
6.70	3.260	10.43	81.50
7.92	3.510	12.64	87.75
11.20	4.060	14.62	101.50
15.80	5.440	19.58	136.00

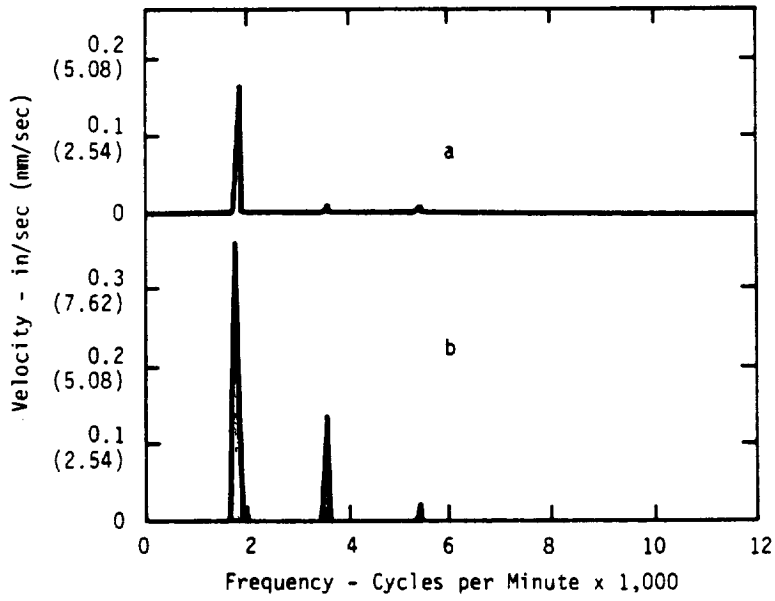

Figure 1. - Vibration signatures of amplitude vs. frequency in a radial direction, a) during normal full load operation, b) during peak vibration subsequent to a thermal down ramp.

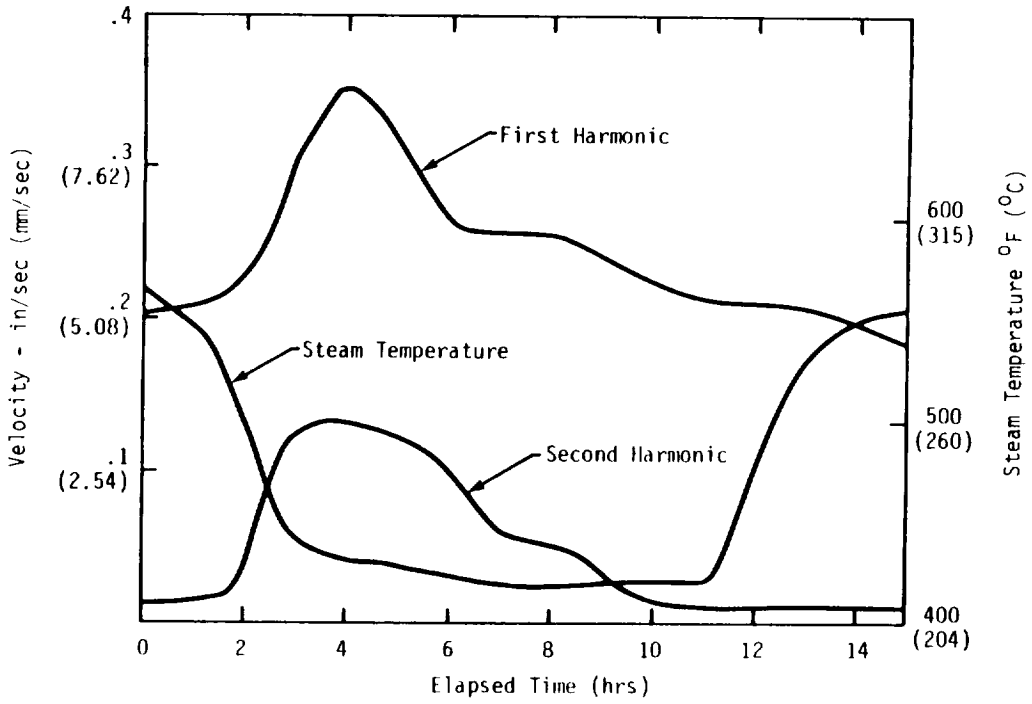

Figure 2. - Vibration amplitude of first and second harmonic and inlet steam temperature vs. time.

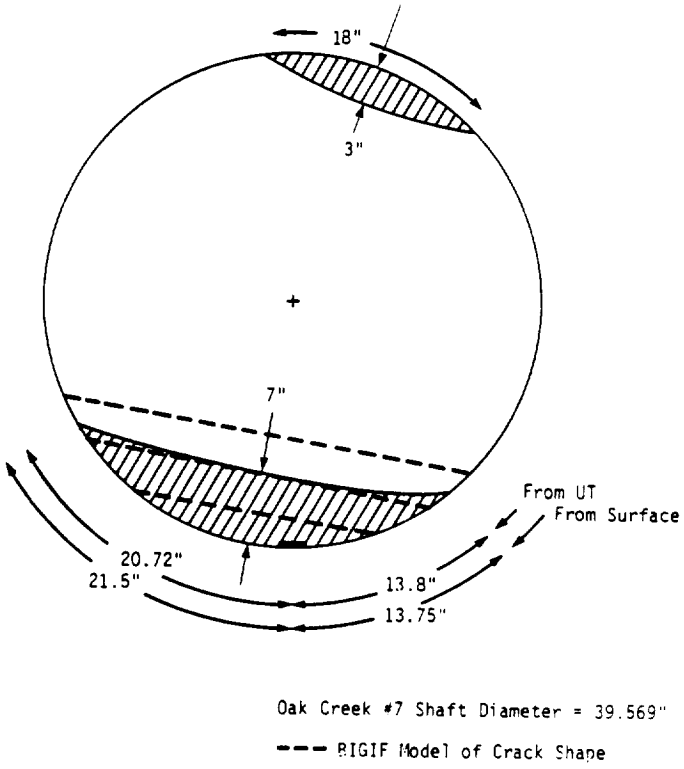

Figure 3. - Representation of Oak Creek #7 LP turbine shaft transverse cracking including BIGIF model.

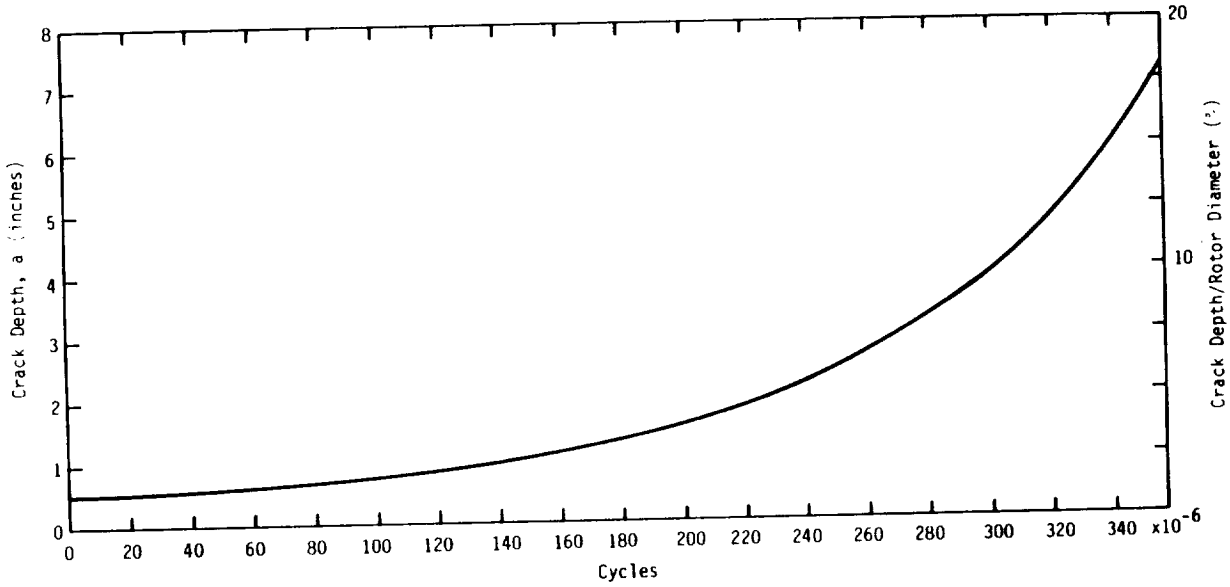

Figure 4. - Transverse crack growth rate due to deslag thermal transients predicted using BIGIF transverse crack model.

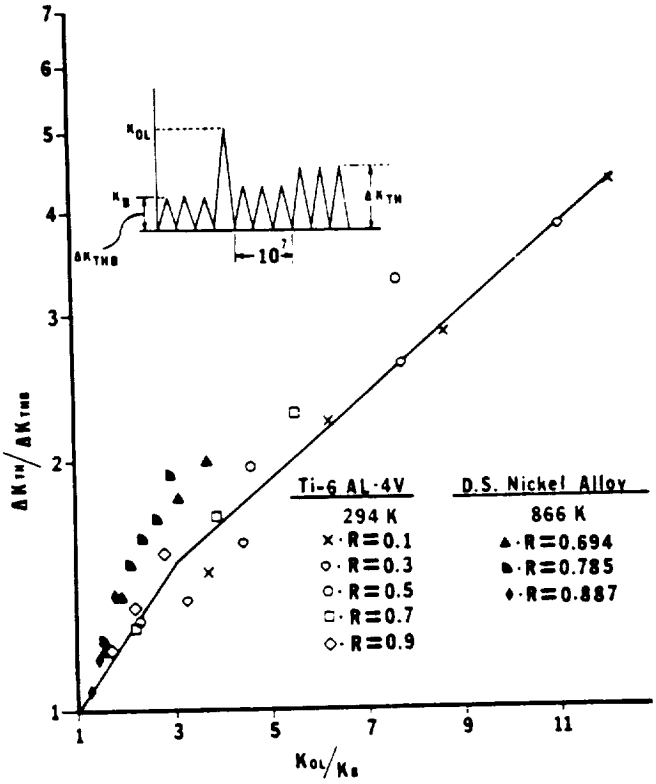

Figure 5. - Relative change in fatigue threshold after single cycle overloads as a function of the relative overload for the alloys and R ratios shown.

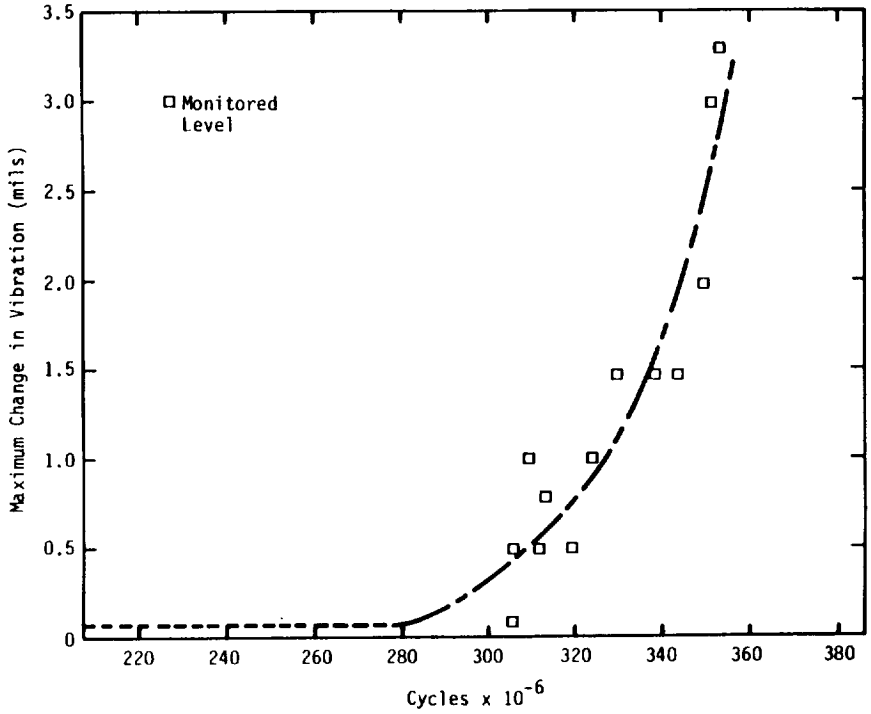

Figure 6. - Maximum changes in LP turbine bearing cap vibration during deslag as a function of total number of cycles at thermal transient stress state.

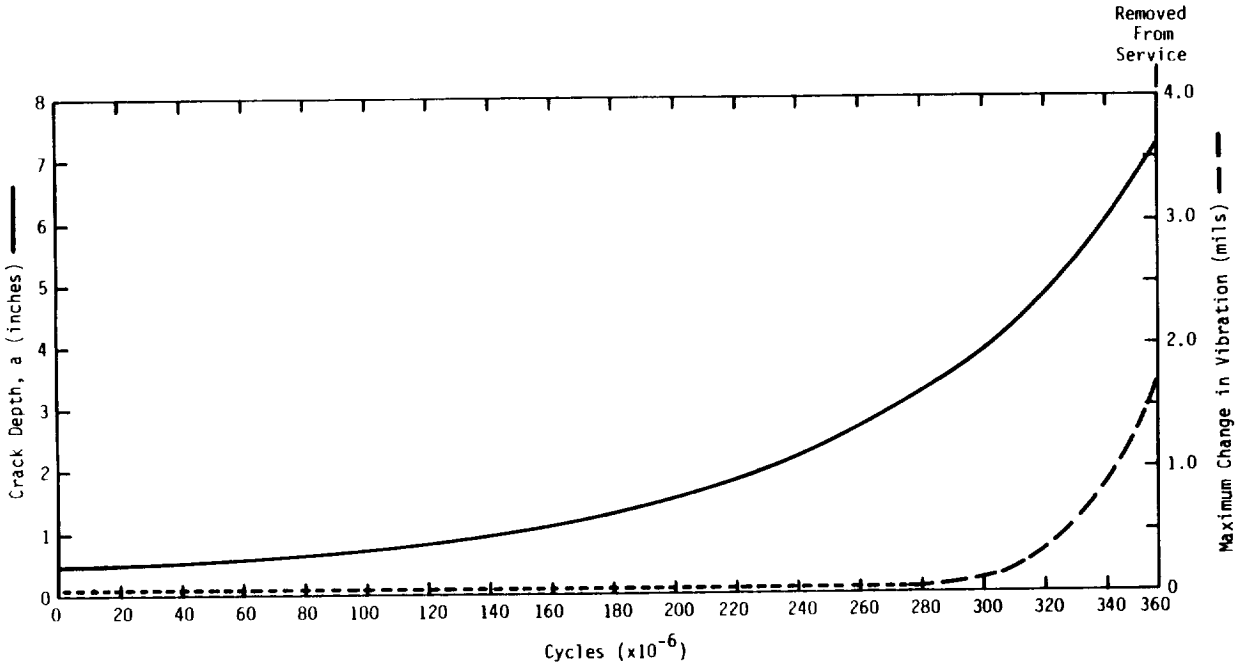

Figure 7. - Correlation of maximum change in LP turbine bearing cap vibration during deslag with predicted rotor crack growth.

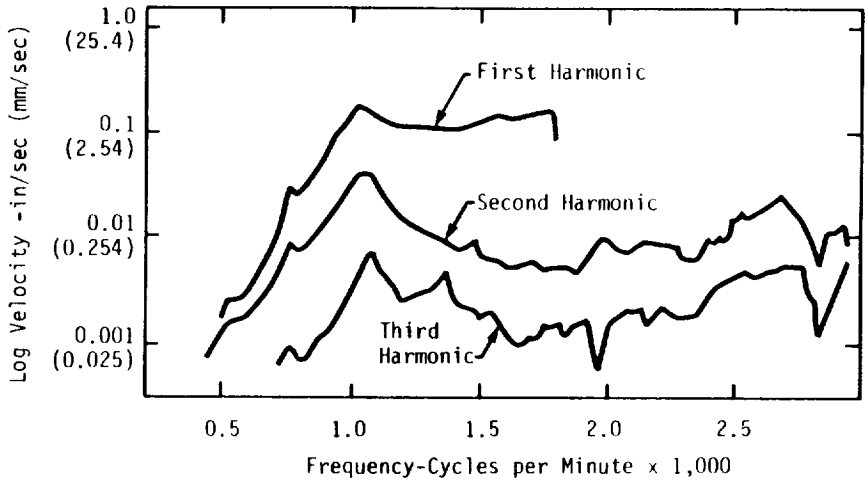

Figure 8. - Bode plot of amplitude vs. frequency for first, second, and third harmonics of running speed.